Local Electrical Properties Tomography With Global Regularization By Gradient

Jiaen Liu[1], Xiaotong Zhang[1], Yicun Wang[1], Pierre-Francois Van de Moortele[2], and Bin He[1,3]
[1]*Biomedical Engineering, University of Minnesota, Minneapolis, Minnesota, United States,* [2]*Center for Magnetic Resonance Research, University of Minnesota, Minneapolis, Minnesota, United States,* [3]*Institute for Engineering in Medicine, University of Minnesota, Minneapolis, Minnesota, United States*

Audience MR Physicists, Radiologists, RF Coil engineers, Electromagnetic model builders, etc.

Purpose With electrical properties tomography (EPT), a recently proposed modality of noninvasively *in vivo* imaging of the electrical conductivity and permittivity of tissues at the Larmor frequency using an MRI scanner, holds significance for both diagnostic purpose and real-time subject-specific local SAR quantification. Traditionally, EPT is derived voxel-wisely using the measurable local B_1 field information. However, the solution of this approach can be severely deteriorated due to noise contamination [1]. In this study, a new approach has been proposed to improve the local EPT solution with the aid of global regularization by the spatial gradient information of electrical properties, which is deducted from the measured transmit B_1 field induced in a multi-channel radiofrequency (RF) coil. Experiments involving a controlled physical phantom and healthy human subject were conducted to evaluate the proposed algorithm.

Theory Using a multi-channel RF coil, the absolute magnitude and relative phase of transmit B_1 field (B_1^+) from individual transmit channels can be measured and used as the input to solve the Maxwell's equations for electrical properties reconstruction [2-5]. Denoting the *relative* B_1 field as $B_{1r}^+ = |B_1^+| e^{i\phi_r}$ and the *absolute* phase of a reference channel as ϕ_0, ignoring the z-component of the B_1 field inside a stripline head array coil which was utilized in the experimental study, the core equation describing the relationship between B_1 field and the electrical properties can be written as eqs. (1) and (2), in which $\varepsilon_c = \varepsilon - i\sigma/\omega$, σ is the conductivity, ε the permittivity, μ_0 the permeability of free space, $\mathbf{g}$ the vector of $\nabla \ln \varepsilon_c$ and $g_+ = g_x + i g_y$. By grouping the unknowns related to ϕ_0 and ε_c into linearly independent components as shown in eqs. (1) and (2), given at least four transmit channels, we can derive $\partial\phi_0/\partial x$, $\partial\phi_0/\partial y$, g_+ and θ. Based on eqs. (1) and (2), the local electrical properties can be calculated voxel-wisely by subtracting the newly solved unknowns from the calculated θ. This local electrical properties solution is denoted as EP_0.

$$\nabla B_{1r}^{+}\cdot\left[2i\nabla\phi_0-\left(g_+,-ig_+,g_z\right)\right]+B_{1r}^{+}\theta\approx-\nabla^2 B_{1r}^{+} \quad (1)$$

$$\theta = i\nabla^2\phi_0-\nabla\phi_0\cdot\nabla\phi_0+\omega^2 u_0\varepsilon_c-i\nabla\phi_0\cdot\left(g_+,-ig_+,g_z\right) \quad (2)$$

$$\min_{\xi}\left[\left|\xi-\xi_0\right|^2+\lambda\left|\left(D_x+iD_y\right)\xi-\mathbf{g}_+\right|^2\right] \quad (3)$$

Methods We propose a global solution of the electrical properties regularized by the derived partial gradient information g_+ as shown in eq. (3). In eq. (3), $\boldsymbol{\xi} = \ln \boldsymbol{\varepsilon}_c$ and $\mathbf{g}_+$ rearrange all the voxels in the region of interest (ROI) into vectors, and D_x and D_y are the differential operation in x- and y-direction, respectively. The regularization coefficient λ is determined by the L-curve method. To evaluate the proposed algorithm, a head-sized gel phantom (diameter of 15 cm and height of 20 cm) with two internal spherical components of a diameter around 3 cm was built as shown in Fig. 2(a), and a healthy human subject was recruited for the *in vivo* experiment following a protocol approved by the university review board. Experiments were conducted on a 7 T scanner (Siemens, Erlangen, Germany). The *relative* complex transmit B_1 fields B_{1r}^+ generated inside a 16-channel transceiver RF coil [6]--with resolution of 1.5x1.5x3 mm^3 for phantom and 1.5x1.5x5 mm^3 for human subject--were obtained using a hybrid B_1-mapping technique [7,8]. To achieve high SNR inside most of the phantom, a CP2+ mode B_1-shimming strategy (stronger in the periphery) [9] was utilized. The measured data were smoothed and utilized to derive EP_0 and g_+ by solving eqs. (1) and (2).

Results Fig. 1 shows the L-curve which was determined in the phantom experiment, and λ of 5 was chosen for both phantom and human studies. Fig. 2 summarizes the result of both local conductivity and global solution after regularization based on eq. (3). In Fig. 2(b), we can observe that the local solution of conductivity is severely affected by noise with structural information hardly identifiable. The results using the proposed algorithm are significantly improved as shown in Fig. 2(d). Table 1 shows a summary of the final conductivity value, in comparison with probe measurement (85070D dielectric probe and E4991A network analyzer, Agilent, Santa Clara, CA, USA) in the phantom and literature report [10] of brain tissues in the human subject.

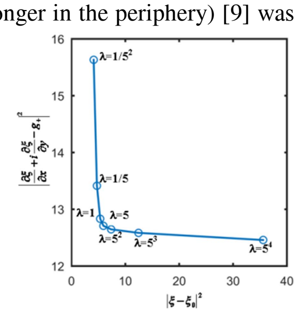

Fig. 1 L-curve determined in the phantom experiment.

Discussion and Conclusion In this study, an algorithm which utilizes partial gradient information about the electrical properties to enhance the local EPT solution was proposed, exhibiting significantly improved reconstruction results in both controlled phantom and *in vivo* human experiment. In a previous study, a gradient-based EPT (gEPT) approach has been developed with elevated robustness against measurement noise and improved reconstruction accuracy in the vicinity of tissue boundaries [5]. Compared to gEPT, the proposed method in this study has two merits: 1) no prior knowledge of electrical property values is required which, on the contrary, is needed in gEPT during spatial integration to derive absolute EP values; 2) only transmit B_1 field is utilized in the calculation, eliminating inconvenient removal of proton density coupled with the receive B_1 maps. It also significantly reduces scanning time and can potentially benefit from fast B_1-mapping techniques towards being practical for clinical applications.

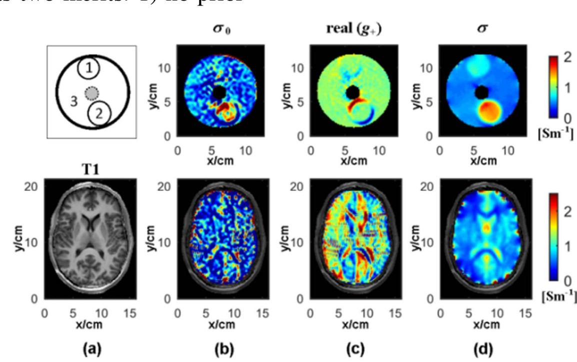

Fig. 2 (a) Phantom structure and T1-weighted image of the brain. (b) Calculated local conductivity σ_0. (c) Real part of calculated g_+. (d) Final global solution of conductivity.

Table 1. Reconstructed conductivity in the phantom and human subject

Phantom			Human Subject		
	Target	Reconstruction		Literature	Reconstruction
#1	0.84	0.74±0.06	WM	0.43	0.51±0.14
#2	1.60	1.38±0.16	GM	0.69	0.69±0.34
#3	0.56	0.50±0.10	CSF	2.22	1.18±0.29

Reference 1. Katscher et al., *IEEE TMI*, 2009, 28:1365; 2. Zhang et al., *MRM*, 2013, 69:1285; 3. Liu et al., *PMB*, 2013, 58:4395; 4. Sodickson et al., *ISMRM* 2012; 5. Liu et al., *MRM*, 2014 online; 6. Adriany et al. *MRM* 2008, 59:590; 7. Van de Moortele et al., *ISMRM* 2007, 1676; 8. Van de Moortele et al., *ISMRM* 2009, 367; 9. Orzada et al., *MRM*, 2013, 70:290; 10. Gabriel et al. *PMB*, 1996, 41: 2271. **Acknowledgement** University of Minnesota Doctoral Dissertation Fellowship, R21 EB017069, R21 EB014353, R01 EB006433, NSF CBET-1450956, P41 EB015894, R01 EB011551, S10 RR026783, WM KECK Foundation